International Journal of Recent Technology and Engineering (IJRTE)
ISSN: 2277-3878 (Online), Volume-8 Issue-2, July 2019

The Effect of Sensor Structure and Coplanar Electrode for Capacitive Based Flow Sensor

Mohd Norzaidi Mat Nawi, Nur Shahira Shahripul Azeman, Muhammad Rashidi Ab Razak

Abstract*: This paper presents the analysis of the capacitive based flow sensor using computational fluid dynamic (CFD) and mathematical equation approach. The CFD simulations for different types of sensor structure were carried out. Pressure and velocity of the fluid were varied in order to study the hydrodynamic parameter such as displacement and drag force. For the coplanar electrode, width of electrode and half gap between electrodes were varied for capacitive response using mathematical approach. Based on the simulation, the displacement of the dome increases as the pressure increases. The result shows that the most suitable thickness of the dome is 0.1 mm based on the displacement and the strain. Meanwhile for the coplanar electrode, the width and half gap showed a significant effect on the capacitance response.

Index Terms*: Capacitive Flow Sensor, CFD, Coplanar Electrode.

I. INTRODUCTION

Underwater surveillance is the requirement to detect, localise and classify targets underwater[1]. Global industries call for technology to be applied in several underwater scenarios such as environmental monitoring and monitoring of underwater structures[2]. Target detection, localization, classification and tracking are some of the issues that need to be considered with surveillance systems[3]. Flow sensors are one of the sensors that are used underwater to measure fluid velocity. There are many types of flow sensors in the flow sensor field which have different functions and purpose. Flow measurement is applied in diverse areas and it is necessary for different engineering operations. There are two commonly used structures in designing a flow sensor which includes the dome-shaped structure [4]. and hair cell structure [5,6].

The Dome-shaped structure of the flow sensor was inspired by the cupula fish which consists of neuromasts[7]. There are two types of neuromasts present in the fish's lateral line, canal and superficial. Both neuromasts have a gelatin cupula which moves according to the flow pressure and induces the neuron signal[8]. A miniature form is cupola (or cupula) which is described as the dome-shaped roof of the pleural cavity that extends into the root of the neck[9]. The common software used in modelling related to fluid is the computational fluid dynamic (CFD) FLUENT software. The FLUENT is able to solve Euler and Navier–Stokes equations in an arbitrary Lagrangian– Eulerian formulation. In this paper, we focus on the simulation of different types of sensor structures using computational fluid dynamic (CFD) approach and mathematical approach for coplanar electrode.

Revised Manuscript Received on 30 July 2019.
***** Correspondence Author
Mohd Norzaidi Mat Nawi*, Department of Physics, Universiti Pendidikan Sultan Idris, Perak, Malaysia.
Nur Shahira Shahripul Azeman, Department of Physics, Universiti Pendidikan Sultan Idris, Perak, Malaysia.
Muhammad Rashidi Ab Razak, Department of Physics, Universiti Pendidikan Sultan Idris, Perak, Malaysia.

II. DESIGN AND METHODOLOGY

A. Analysis Sensor Structure using CFD

Computational fluid dynamics (CFD) is an effective and powerful tool that stimulates fluid flow numerically[10]. Besides that, computational fluid dynamics (CFD) is an interdisciplinary tool that is related to both the computer technology and fluid physics[11]. Capacitive based flow sensor needs the CFD simulation approach to get an effective simulation and to produce the best result especially on drag force acting on the different types of structures. There are a few steps involved in the CFD simulation process for modelling structure. Fig. 1 shows the CFD simulation process.

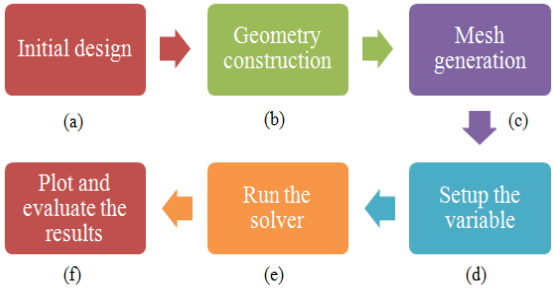

Fig. 1: CFD Simulation process. (a) Dome-shape is selected as the initial design. (b) Designed the dome-shaped structure in Solidwork 2016 and is imported to ANSYS Fluent. (c) Mesh is applied on the dome-shaped structure. (d) Setup the variable to test the design structure. (e) Run the solver to get the result (f) The data obtained are collected and inserted into the table.

The CFD simulation process needs to be carried out in order to run the simulation and test different types of microfluidics flow sensor structure including structure of dome, ellipse and hair cell. Different types of structures needed to be designed and imported into the ANSYS Fluent 18.1. Then, mesh was applied on the design before setting up the variable. Each faces of the design were labelled based on its function, such as input and output.

Then, variable such as velocity showed a variation of 1 m/s to 10 m/s which is suitable for robust application[12]. The iteration number was set up to 100 for sequence of outcome generation. The results of the three design structure simulation is shown in Fig. 2 (a), (b) and (c).

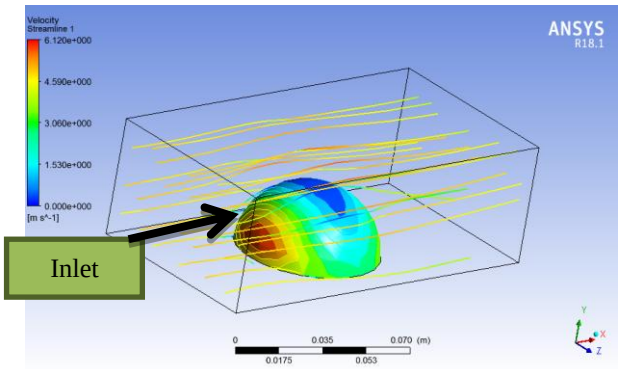

(a)

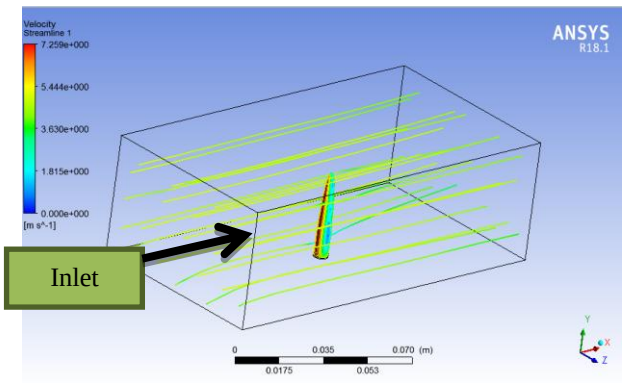

(b)

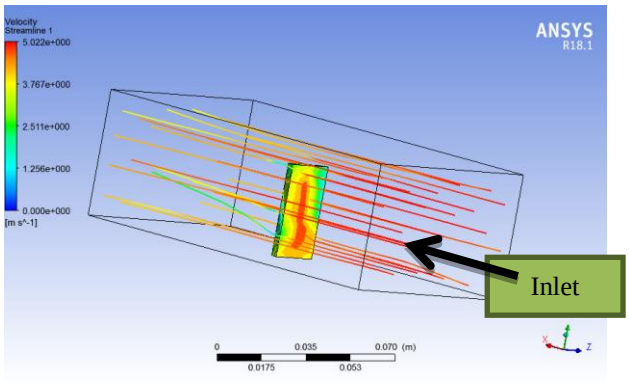

(c)

Fig. 2 (a) Streamline of dome; (b): Streamline of ellipse; (c) Streamline of hair cell

Fig. 2 (a), (b) and (c) shows the velocity streamline of dome, ellipse and hair cell structures that have been simulated. All of these three figures show velocity that pass through three different structures. Fig. 2 (a) shows yellow and green velocity along the streamline and it shows low air resistance of ellipse structure based on the velocity streamline guide level in m/s. Fig. 2 (b) shows orange at the inlet, red at the center, yellow and green at the outlet of the velocity streamline. It shows that high air resistance at the beginning of the streamline and low air resistance at the end of the streamline. Next, fig. 2 (c) shows red at the inlet, green and yellow at the outlet. It shows that hair cell has very high air resistance at the beginning of the streamline and low air resistance at the end of streamline.

B. Coplanar Electrode Design

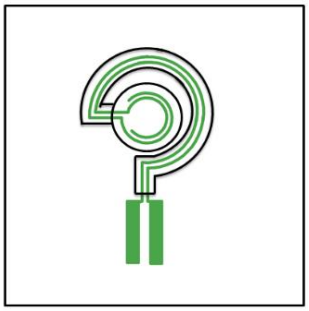

(a)

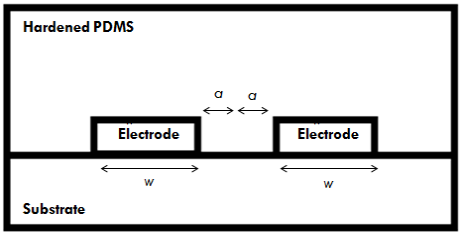

(b)

Fig. 3 (a) Electrode pattern with implementation of coplanar design; (b) cross section of microchannel

Fig. 3 (a) shows the proposed electrode pattern located under flow sensor structure. Electrode findings do not use any software to run simulation. Electrode was analyzed using a mathematical equation to determine the capacitive response. The equation that was used as a guideline to optimize the electrode dimension is from a previous research. . In this research, capacitance formula by Chen et al.,[13] was applied to find the capacitive response of the electrode. Width of electrode and half gap between electrodes were varied as Equation 1 shows the capacitive response

$$c = \frac{2\varepsilon_r \varepsilon_0 l}{\pi} \ln\left[\left(1+\frac{w}{a}\right)+\sqrt{\left(1+\frac{w}{a}\right)^2-1}\right] \quad (1)$$

C, ε_r, ε_o, w and a are constant variables. The liquid that was involved in the mathematical approach is propylene carbonate (PC) which has 66.2 dielectric constants. Width of electrode, w was varied from 0.01 mm to 0.10 mm. Capacitance values show increasing linearly results. Half gap between electrodes, were varied from 0.05 mm to 0.5 mm and capacitance values shows decreasing results. The microchannel contains two electrodes called coplanar electrode, substrate at the bottom and hardened PDMS on top. The cross sections of electrode inside microchannel are as shown in Fig. 3(b).

III. RESULT AND DISCUSSION

The findings obtained from ANSYS Fluent 18.1 and mathematical approach by capacitive equation..

A. CFD Simulation

Three different structures were simulated using the ANSYS Fluent 18.1 and the results were obtained. Three different structures which are ellipse, dome and hair cell structures had been created to be tested based on drag force. Fig. 4 shows the findings of the drag force acting on different types of structures.

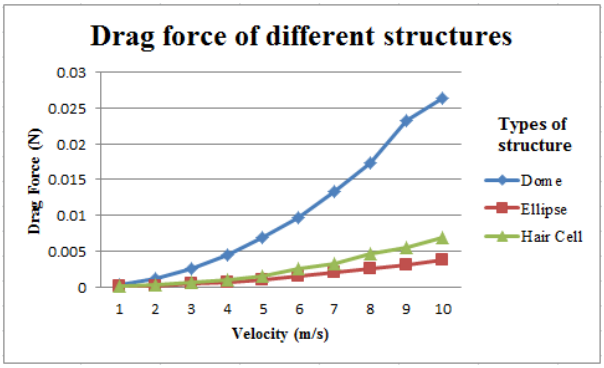

Fig 4: Drag force of different types of structures

Velocity was varied from 1 m/s to 10 m/s to test different types of structures. Velocity along trace lines reporting velocities as large as 10 m/s. This shows that the most suitable velocity for robust application is 10 m/s. For that reason, velocity in the range between 1 m/s to 10 m/s was used for the simulation/simulations. The graph shows that the dome structure produces the highest value of drag force acting on the structures compared to hair cell and ellipse structure. It also shows that the dome structure has a regular shape that gives uniform velocity around the structure compared to hair cell and ellipse.

B. Output Response for Coplanar Electrode

In designing an electrode, the mathematical equation approach was applied to obtain the output response in capacitance. In equation 1, there are two variables that act as constant variables which are width, *w* and half gap between two electrodes, *a*. There are three results that correspond to these two constant variables.

A. Width of electrode, w constant

The width of electrode was fixed at 0.1 mm. The liquid that was used in this research is propylene carbonate (PC) and its dielectric constant, ε_r is 66.2. Table I shows the data of the capacitive response when w is constant.

Then, all the data was transferred into graphs. Two graphs were built based on Table 1. The first one is the correspondence between width to aspect ratio, w/a and capacitance per unit length as shown in Fig. 5. It shows that when width to aspect ratio increased, capacitance per unit length decreased. The highest capacitance per unit length is when the width to aspect ratio is 2 and the lowest capacitance per unit length is when width to aspect ratio is 0.2. The second graph that was built from table 1 is correspondence between capacitance per unit length and half gap between electrode, a. Figure 5 shows the capacitance result of different half gap.

TABLE I. The data result when *w* is constant

half gap between electrode, *a* (mm)	width to aspect ratio, *w/a*	Capacitance (F)	capacitance per unit length, *C/l*(F/mm)
0.05	2.000	1.98E-08	6.01E-10
0.10	1.000	1.35E-08	4.10E-10
0.15	0.667	1.04E-08	3.16E-10
0.20	0.500	8.54E-09	2.59E-10
0.25	0.400	7.24E-09	2.19E-10
0.30	0.333	6.29E-09	1.90E-10
0.35	0.286	5.57E-09	1.69E-10
0.40	0.250	4.99E-09	1.51E-10
0.45	0.222	4.52E-09	1.37E-10
0.50	0.200	4.14E-09	1.26E-10

Then, all the data was transferred into graphs. T Two graphs were built based on Table 1. The first one is the correspondence between width to aspect ratio, w/a and capacitance per unit length as shown in Fig. 5. It shows that when width to aspect ratio increased, capacitance per unit length decreased. The highest capacitance per unit length is when the width to aspect ratio is 2 and the lowest capacitance per unit length is when width to aspect ratio is 0.2. The second graph that was built from table 1 is correspondence between capacitance per unit length and half gap between electrode, a. Figure 5 shows the capacitance result of different half gap.

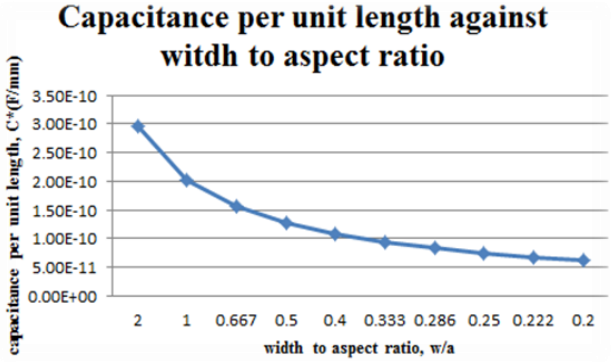

Fig. 5: The capacitance result of different to aspect ratio

Fig. 6 shows that when half gap between electrodes becomes larger the capacitance per unit length increases. The value of capacitance per unit length when at the smallest half gap between electrodes is 6.00 x 10^{10} F/mm, while the value of capacitance per unit length is at the largest gap which is about 1.00 x 10^{10} F/mm.

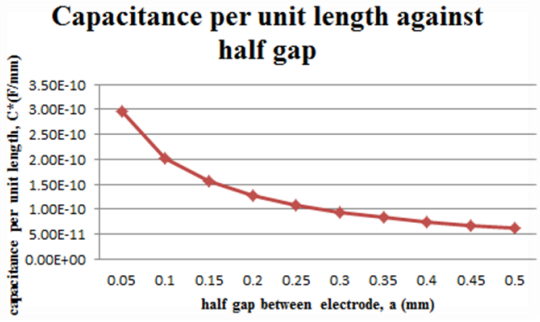

Fig. 6: The capacitance result of different half gap between electrodes

B. Half gap between electrodes, a constant

Half gap between electrodes was fixed at 0.24 mm. Table 2 shows the capacitive response data of different width of electrode, *w*.

TABLE II. The data of capacitive response

width, *w* (mm)	Capacitance, *C* (F)	Capacitance per unit length, *C/l*(F/mm)
0.01	9.48E-10	2.87E-11
0.02	1.83E-09	5.54E-11
0.03	2.65E-09	8.03E-11
0.04	3.42E-09	1.04E-10
0.05	4.14E-09	1.26E-10
0.06	4.83E-09	1.46E-10
0.07	5.48E-09	1.66E-10
0.08	6.09E-09	1.85E-10
0.09	6.68E-09	2.02E-10
0.10	7.24E-09	2.19E-10

All the data in table II were obtained from the mathematical equation of capacitive response due to the different value of width of electrode, *w* and constant of half gap between electrodes. Then the data was transfered into the graph that is shown in Fig. 7.

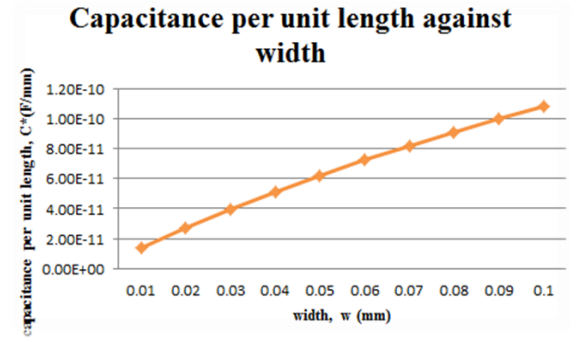

Fig. 7: Capacitance per unit length depends on scale of width

Fig. 7 shows capacitance per unit length value based on the width value. The graph shows capacitance per unit length increased linearly to the width of electrode, *w*. The highest capacitance per unit length is when the width of electrode is 0.1 mm and the lowest capacitance per unit length is when the width of electrode is 0.01 mm.

IV. CONCLUSION AND FUTURE SCOPE

CFD simulation work on different types of flow sensor structures was successful. The result shows that a dome structure produces the highest value of drag force compared to hair cell structure and ellipse structure based on the velocity. For coplanar electrode, the larger the width of the electrode the higher the capacitance per unit length increases while the larger the half gap between electrodes, the lower the capacitance per unit length decreases. This consideration of electrode dimension is important when designing the capacitive based flow sensor.

ACKNOWLEDGMENT

This research has been carried out under University Research Grants Scheme UPSI (2016-0180-102-01) and Fundamental Research Grants Scheme (2017-0077-101-02).

REFERENCES

1. Ferri, G., Munafò, A., Tesei, A., Braca, P., Meyer, F., Pelekanakis, K., Petroccia, R., Alves, J., Strode, C. and LePage, K., 2017. Cooperative robotic networks for underwater surveillance: an overview. *IET Radar, Sonar & Navigation*, 11(12), pp.1740-1761.
2. Hasan, N., Sefat, M.S. and Shahjahan, M., 2017, February. A low cost remotely operated vehicle for underwater surveillance—A complete experimental platform. In 2017 *IEEE International Conference on Electrical, Computer and Communication Engineering (ECCE)* (pp. 486-490).
3. Munasinghe, K., Aseeri, M., Almorqi, S., Hossain, M., Binte Wali, M. and Jamalipour, A., 2017. EM-based high speed wireless sensor networks for underwater surveillance and target tracking. *Journal of Sensors*, 2017.
4. Asadnia M., Kottapalli A.G.P., Karavitaki K.D., Warkiani M.E., Miao J., Corey D.P. & Triantafyllou M.(2016). From Biological Cilia to Artificial Flow Sensors: Biomimetic Soft Polymer Nanosensors with High Sensing Performance. *Scientific Reports*.
5. Qualtieri, A., Rizzi, F., Todaro, M.T., Passaseo, A., Cingolani, R., and De Vittorio, M. (2011). Stress-driven AlN cantilever-based flow sensor for fish lateral line system. *Microelectronic Engineering*. 88(8): 2376-2378.
6. Sadeghi, M.M., Peterson, R.L., and Najafi, K. (2013). A 2-D directional air flow sensor array made using stereolithography and MEMS micro-hydraulic structures. *The 17th International Conference on Solid-State Sensors, Actuators and Microsystems* (TRANSDUCERS & EUROSENSORS XXVII). 722-725.
7. Nawi, M.N.M., Manaf, A.A., Arshad, M.R. and Sidek, O., 2012. Modeling of biomimetic flow sensor based on artificial hair cell using CFD and FEM Approach. *In Proceeding Conference on Simulation of Semiconductor Processes and Devices (SISPAD 2012)* (pp. 161-164).
8. A.J. Hudspeth, Y. Choe, A.D. Mehta, P. Martin, "Putting ion channels to work: Mechanoelectrical transduction, adaptation, and amplification by hair cells", *Proceedings of the National Academy of Sciences of the United States of America*, 97, pp. 11765- 11772, 2000.
9. Robert Fortuine, 2000. THE WORDS OF MEDICINE: Sources, Meanings, and Delights. 0398083134, 9780398083137.The Imagery of Medicine: Home and Earth m/s 139. Charles C Thomas Publisher, LTD. 2600, South First Street, Springfield. Illinois 62704, USA.
10. Hosain, M.L. and Fdhila, R.B., 2015. Literature review of accelerated CFD simulation methods towards online application. *Energy Procedia*, 75, pp.3307-3314.
11. Lu, J., Yu, J., & Shi, H. ,2017. Feasibility Study of Computational Fluid Dynamics Simulation of Coronary Computed Tomography Angiography Based on Dual-Source Computed Tomography. *Journal of Clinical Medicine Research*, 9(1), 40–45.
12. Magirl, C. S., Gartner, J. W., Smart, G. M., & Webb, R. H., 2009. Water velocity and the nature of critical flow in large rapids on the Colorado River, Utah. *Water Resources Research*, 45(5).

13. Chen, J.Z., Darhuber, A.A., Troian, S.M. and Wagner, S., 2004. Capacitive sensing of droplets for microfluidic devices based on thermocapillary actuation. *Lab on a Chip*, 4(5), pp.473-480.

AUTHORS PROFILE

Mohd Norzaidi Mat Nawi received the B.Eng. degree in Mechatronic Engineering from the Universiti Sains Malaysia, Nibong Tebal, Malaysia in 2010, and the Ph.D degree in electrical and electronic engineering with a specialization in Fluidic based flow sensor in 2015. He is currently interested in designing low cost flow sensor for underwater robotic applications.

Nur Shahira Shahripul Azeman received the B.Education degree in physics education from Universiti Pendidikan Sultan Idris, Perak, Malaysia, in 2017 where she is currently pursuing the M.Sc in Physics. Her research focuses on the fluidic-based sensor for flow measurement. She is well versed in microelectromechanical systems design software such as Ansys and Autodesk Inventor Professional.

Muhammad Rashidi Ab Razak received the B.Eng. degree in Electrical Engineering from Universiti Malaysia Pahang, Pahang, Malaysia in 2015. He is currently pursuing the MSc in Physics from Universiti Pendidikan Sultan Idris, Perak, Malaysia. His research focuses on the fluidic-based sensor for pressure applications.